Tissue reservoirs of antiviral T cell immunity in persistent human CMV infection

Claire L. Gordon,[1,4] Michelle Miron,[1,2] Joseph J.C. Thome,[1,2] Nobuhide Matsuoka,[1] Joshua Weiner,[1] Michael A. Rak,[5] Suzu Igarashi,[5] Tomer Granot,[1] Harvey Lerner,[6] Felicia Goodrum,[5] and Donna L. Farber[1,2,3]

[1]Columbia Center for Translational Immunology, [2]Department of Microbiology and Immunology, [3]Department of Surgery, and [4]Department of Medicine, Columbia University Medical Center, New York, NY 10032
[5]Department of Immunobiology, University of Arizona, Tucson, AZ 85721
[6]LiveOnNY, New York, NY 10001

T cell responses to viruses are initiated and maintained in tissue sites; however, knowledge of human antiviral T cells is largely derived from blood. Cytomegalovirus (CMV) persists in most humans, requires T cell immunity to control, yet tissue immune responses remain undefined. Here, we investigated human CMV–specific T cells, virus persistence and CMV–associated T cell homeostasis in blood, lymphoid, mucosal and secretory tissues of 44 CMV seropositive and 28 seronegative donors. CMV–specific T cells were maintained in distinct distribution patterns, highest in blood, bone marrow (BM), or lymph nodes (LN), with the frequency and function in blood distinct from tissues. CMV genomes were detected predominantly in lung and also in spleen, BM, blood and LN. High frequencies of activated CMV–specific T cells were found in blood and BM samples with low virus detection, whereas in lung, CMV–specific T cells were present along with detectable virus. In LNs, CMV–specific T cells exhibited quiescent phenotypes independent of virus. Overall, T cell differentiation was enhanced in sites of viral persistence with age. Together, our results suggest tissue T cell reservoirs for CMV control shaped by both viral and tissue–intrinsic factors, with global effects on homeostasis of tissue T cells over the lifespan.

INTRODUCTION

T cell responses to viruses are initiated, function, and are maintained as memory subsets in diverse tissues sites. Studies in mouse models have revealed the importance of tissue-localized T cell responses in viral clearance and indicate that long-term T cell immunity is maintained both as circulating and tissue-resident populations (Masopust et al., 2001, 2004, 2006; Kivisäkk et al., 2003; Bingaman et al., 2005; Tokoyoda et al., 2009; Wakim et al., 2010). In mouse infection models, noncirculating, tissue–resident memory (TRM) T cells are generated in diverse sites in response to acute and chronic viruses, including influenza (lungs), murine cytomegalovirus (MCMV; salivary glands), lymphocytic choriomeningitis virus (LCMV; many sites), and HSV (skin and vaginal mucosa; Gebhardt et al., 2009; Teijaro et al., 2011; Anderson et al., 2012; Turner et al., 2014; Smith et al., 2015; Thom et al., 2015). Although TRM can mediate optimal protective responses to site-specific reinfection (Liu et al., 2010; Jiang et al., 2012; Iijima and Iwasaki, 2014; Schenkel et al., 2014), circulating memory subsets can mediate protection to systemic viruses (Wherry et al., 2003; Xu et al., 2007). Factors determining whether antiviral memory T cells are maintained as circulating and/or tissue-localized populations remain undefined.

The diverse tissue localization of long term T cell–mediated immunity is difficult to study in humans, where sampling is largely limited to peripheral blood which comprises an estimated 2–3% of total body T cells (Ganusov and De Boer, 2007). Furthermore, the discovery of TRM indicates that the circulating T cell response as studied in humans may not accurately reflect the quantity or quality of virus-specific T cell responses in tissues. Addressing this fundamental question in human immunology requires obtaining blood and multiple tissues from individuals during a dynamic response to virus infection—a challenge that has previously been impossible to overcome.

We have set up a novel tissue resource and protocol with the organ procurement organization for New York City to obtain multiple lymphoid and mucosal tissues from diverse individual organ donors, providing an unprecedented opportunity to study immune cells and responses in tissues and circulation. Through optimization and study of T cells in these tissue samples, we have discovered novel aspects of how human T cells differentiate, become compartmentalized and function in tissues and circulation at different life stages (Thome et al., 2014, 2016). These tissues also provide a new opportunity to study ongoing antiviral T cell responses in situ,

as the donor profile indicates seropositivity for the prevalent persisting herpesviruses, human cytomegalovirus (hCMV; 60% donors), and/or Epstein-Barr Virus (EBV; 85% donors). Notably, human CMV requires active T cell responses to be controlled—a significant proportion of blood CD8^{+} T cells (5–30%) are CMV-specific in seropositive individuals, suggesting that much of the human T cell response is being diverted to control CMV, and maintain the virus in a latent form (Polić et al., 1998; Gamadia et al., 2001). Examining CMV-specific T cells in these tissues therefore provides a unique opportunity to examine dynamic virus-specific human T cell responses in diverse sites from individuals of all ages.

Persistent CMV infection has important clinical relevance in the global population. Although immune-mediated control of CMV in healthy individuals prevents disease and overt clinical symptoms, immune dysregulation caused by immunosuppressive treatments in transplant and cancer patients, congenital immunodeficiencies, HIV/AIDS, and/or aging can result in CMV viremia, life threatening disease, and even death (Ljungman et al., 2010; Kotton et al., 2013; Frantzeskaki et al., 2015; Lichtner et al., 2015). When reactivated, CMV infects multiple tissues, causing pneumonitis, colitis, hepatitis, and end organ failure (Ljungman et al., 2010; Kotton et al., 2013), for which antiviral therapeutics are only partially effective. CMV persistence may also impact immunity in immunocompetent individuals, and has been associated with immunosenesence, and differential responses to infections or vaccinations (Pera et al., 2014; Arens et al., 2015; Furman et al., 2015). The dynamic nature of viral persistence and antiviral T cell responses indicates that both parameters need to be investigated to understand the mechanisms for immune-mediated escape and/or other effects on overall immune homeostasis.

Here, we present a novel analysis of CMV-specific T cell responses, CMV persistence, and T cell homeostasis in blood, primary and secondary lymphoid tissues (BM, spleen, and multiple LNs), and mucosal sites (lungs and intestines) of CMV-seropositive (44) and –seronegative (28) donors spanning seven decades of human life. CMV-specific CD8 T cells were detected in multiple tissues of seropositive donors including significant frequencies in the lungs, negligible frequencies in the intestines, with the highest frequencies found either in blood, BM, or LN compared with other sites within the same individual. The activation and functional profile of CMV-specific T cells related to their frequency distribution pattern, tissue, and subset. CMV viral genomes were detected in the majority of CMV-seropositive lungs, followed by LNs, and rarely in blood or BM from individuals with high frequency T cell responses with activation profiles in these sites, suggestive of local viral control. In the major sites of CMV-specific T cell responses and CMV persistence, CMV-seropositive donors exhibited accelerated polyclonal T cell differentiation into terminal effectors or effector-memory subsets with age compared with seronegative donors. Together, our results reveal tissue-specific effects on the maintenance of antiviral T cell immunity with impacts on virus persistence and T cell homeostasis over the human lifespan.

RESULTS

Heterogeneous distribution of CMV–specific CD8^{+} T cells in diverse tissue sites

Lymphoid and mucosal tissues were obtained from research-consented human organ donors through a collaboration and research protocol with LiveOnNY as previously described (Sathaliyawala et al., 2013; Thome et al., 2014). All donors were healthy (HIV[−], HBV/HCV[−], cancer-free, and free of systemic infections) before brain death, with information on HLA-typing and CMV/EBV serology available. For analysis of CMV immunity and persistence in tissues, we analyzed multiple anatomical sites (blood, BM, spleen, peripheral, and mucosal-draining lymph nodes, lungs, and intestines) from a cohort of 41 donors (24 seropositive and 17 seronegative), aged 6–70 yr (Table 1). Donors had been hospitalized for a median of 5.5 d (interquartile range, 5.5–6.5 d) and had died from traumatic causes including head trauma (33%), anoxia (25%), or cerebrovascular event/stoke (42%), which all resulted in brain death. Additional analysis of donor serum from seropositive individuals revealed the presence of high and intermediate avidity CMV-specific IgG and the absence of IgM anti-CMV antibodies, consistent with remote primary CMV infection with no evidence of current reactivation (Table 1).

We screened for the presence of CMV-specific CD8^{+} T cells in tissues from seropositive donors using up to five HLA tetramer or multimer reagents of the appropriate HLA type (Table S1), containing peptide epitopes of immunodominant CMV proteins pp65, IE-1, and pp50 (CMV multimers), compared with staining with negative control HLA-multimers (Fig. 1 A and Fig. S1). We used combinations of CMV multimers containing different CMV epitopes to maximize our ability to detect CMV-reactive T cells in each sites; however, we also stained with single multimer reagents to measure the distribution of CD8^{+} T cells specific for single peptide epitopes across tissues (Table 2). CD8^{+} T cells obtained from 20/24 seropositive donors exhibited significant CMV multimer–binding frequencies above negative controls (>0.1–0.3% of CD8^{+} T cells; Figs. 1 A and S1), although tissue T cells from seronegative donors had negligible frequencies of CMV multimer^{+} CD8^{+} T cells (Fig. 1 A). The frequency of CMV multimer^{+} T cells was similar to the frequency of CD8^{+} T cells responding to 6-h stimulation with immunodominant CMV peptide epitopes of pp65 and IE-1, as measured by IFN-γ production and up-regulation of the activation marker CD69 (Fig. 1 B). This concordance of multimer staining with peptide–specific responses is consistent with previous studies validating the use of HLA-peptide multimer reagents to quantitate virus-specific T cells (Borchers et al., 2014).

We assessed qualitative and quantitative aspects of CMV-specific CD8^{+} T cell tissue distribution within and between the 20 seropositive donors with detectable multimer frequencies (Table 2). Overall, CMV-specific CD8^{+} T cells were consistently detected in multiple sites includ-

ing blood, BM, several LNs, and lungs, whereas negligible frequencies were detected in the intestines (Fig. 1 and Table 2). Quantitatively, however, there was heterogeneity in the frequency and distribution of CMV-specific (multimer^{+}) CD8^{+} T cells between tissue sites of individual donors (Fig. 1 A). In 16/20 donors, there were notable high frequencies biased to specific tissue sites, with some donors having highest frequencies in blood compared with other sites ($n = 4$; 20% donors), others in BM ($n = 9$; 45% donors), and others with highest frequencies in LNs ($n =$ 3; 15% donors; Fig. 1, A and C). In addition, 4/20 donors (20%) showed no tissue bias in CMV-specific T cell distribution, exhibiting comparable low frequencies in multiple sites (Fig. 1, A and C). Our findings of maximum frequencies within specific sites were observed with CMV-specific T cells specific for single epitopes, or when multiple specificities were assessed (Table 2). In all donors, the frequency of CD8^{+} T cells specific for single or combined epitopes of CMV in peripheral blood was not representative of their frequency in tissues.

Table 1. **Characteristics of organ donors from which tissues were obtained for this study**

Donor	Age	Sex	Cause of death	Length of stay	EBV IgG	CMV IgG	CMV IgG avidity[a]	CMV IgM[b]	HLA type	CMV–multimer detected[c]
	yr			d						
201	21	M	HT	7	+	+	High	−	A2, B7	Yes
146	23	F	HT	5	+	+	ND	ND	A2	Yes
207	23	M	HT	7	+	+	High	−	A2	Yes
103	25	M	HT	7	+	+	High	−	A3, B35	Yes
227	26	M	HT	20	+	+	High	−	A3	Yes
204	30	M	CVA	3	+	+	Low	−	A3	No
169	33	M	HT	3	ND	+	ND	ND	A3, A24	Yes
216	34	M	HT	6	+	+	ND	ND	A2	Yes
174	35	F	A	7	+	+	ND	ND	A3, B7	Yes
147	36	F	CVA	10	+	+	ND	ND	A2, A24	Yes
195	37	F	CVA	4	+	+	I	−	A2, B35	No
150	39	M	CVA	5	+	+	High	−	A24, B35	Yes
156	40	F	CVA	5	+	+	ND	ND	A2, A24	Yes
196	45	F	CVA	9	+	+	High	−	A2	Yes
172	49	M	A	6	+	+	High	−	A24, A68, B7	Yes
217	49	M	A	5	+	+	High	−	A68, B7	Yes
199	50	M	CVA	15	+	+	High	−	A2, A3	Yes
194	53	M	CVA	12	+	+	High	−	A24, B7	Yes
208	54	M	A	5	+	+	I	−	A3, A24, B7	Yes
225	54	M	CVA	5	−	+	High	−	A24	No
220	64	M	A	3	+	+	High	−	A2, A24	Yes
226	66	F	HT	4	+	+	ND	ND	A1, A3, B35	Yes
190	69	F	CVA	5	+	+	I	−	A68	No
197	70	F	A	8	+	+	ND	ND	A1	Yes
143	6	M	CVA	2	+	−	ND	ND	A2, A3, B7	No
105	20	M	HT	11	+	−	ND	ND	A2, A24	No
86	24	F	HT	11	+	−	ND	ND	A24	No
84	31	F	A	3	+	−	ND	ND	A1, A2, B35	No
39	32	M	NA	NA	+	−	ND	ND	A3	No
48	35	M	HT	3	+	−	ND	ND	B35	No
83	41	M	CVA	9	+	−	ND	ND	A2, B7	No
81	43	M	CVA	2	+	−	ND	ND	A2, B7	No
212	48	M	NA	NA	+	−	ND	ND	A2, B7	No
193	50	M	A	23	+	−	ND	ND	A24	No
202	50	M	CVA	6	+	−	ND	ND	A3, B7	No
206	50	M	CVA	8	+	−	ND	ND	A1	No
177	52	F	CVA	3	+	−	ND	ND	A2	No
200	55	M	CVA	7	+	−	ND	ND	A2, B7	No
111	58	M	CVA	3	+	−	ND	ND	A1, A2	No
209	59	M	CVA	4	+	−	ND	ND	A2	No
65	69	M	CVA	6	+	−	ND	ND	A68	No

−, negative; +, positive; NA, not available; ND, not done; F, female; HLA, human leukocyte antigen; M, male.
[a]CMV IgG avidity index reference ranges: High (≥0.60), intermediate (0.51–0.59), low (≤0.50).
[b]CMV IgM reference range: Negative (≤0.80), equivocal (0.9–1.0), positive (≥1.1).
[c]CMV–multimer detected is defined as >0.1–0.3% of CD8^{+} T cells where >500 CD8^{+} T cells were available.
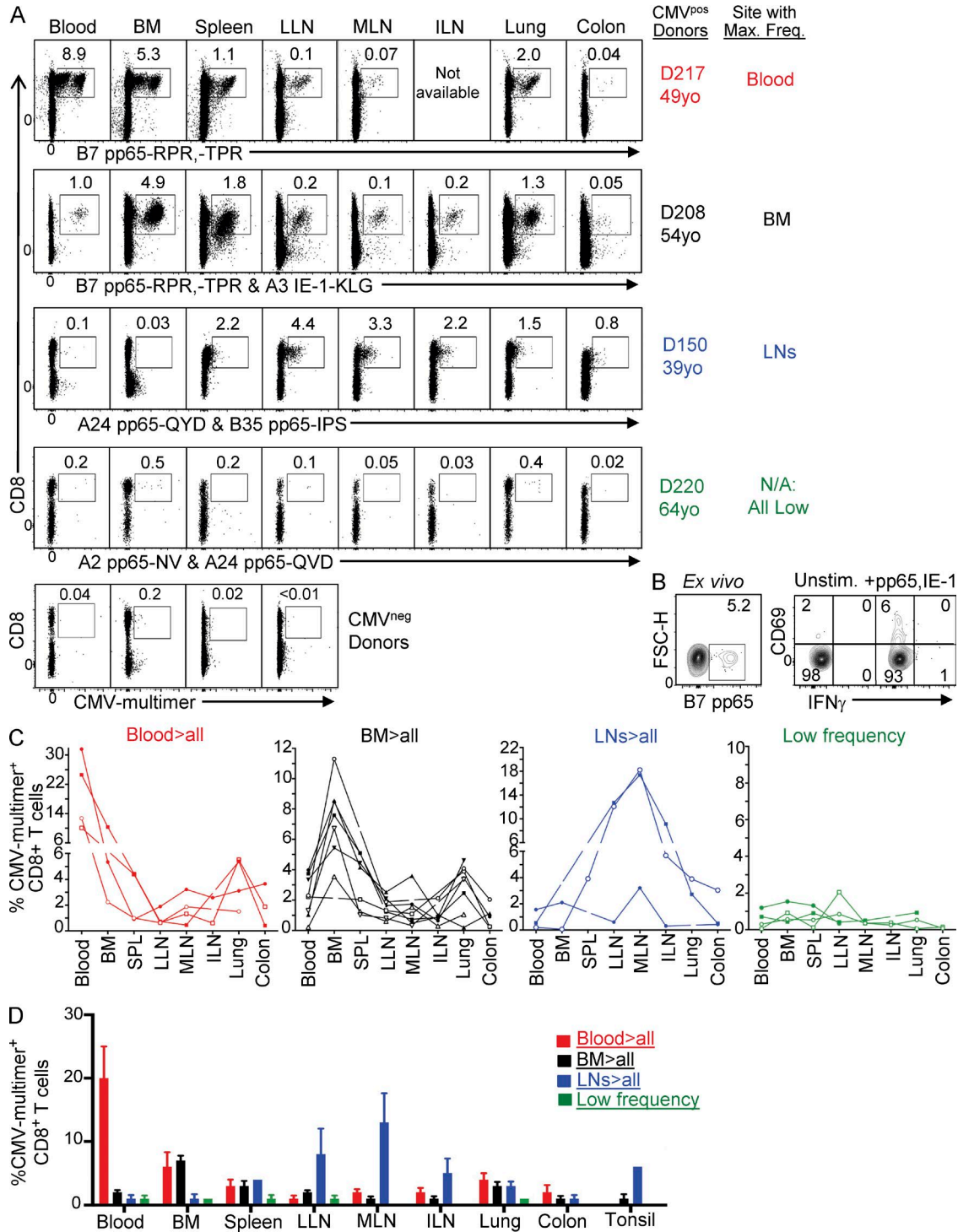
Figure 1. **Heterogeneity of CMV–specific CD8⁺ T cell distribution in circulation and tissues.** CMV-specific CD8⁺ T cell distribution was assessed by staining with HLA multimer reagents containing CMV-specific epitopes (CMV-multimers; see Table S1 for complete list) from 24 CMV-seropositive and 17 CMV-seronegative organ donors aged 6–70 yr. (A) Representative flow cytometry plots of CMV-multimer staining of live CD3⁺CD19⁻CD4⁻CD8⁺ cells in blood and indicated tissues (BM, LLN, MLN, and ILN) gated based on staining with negative multimer controls (see Materials and methods) from four representative CMV-seropositive individual donors (top four rows) and four representative CMV-seronegative donors (bottom row). Individual donors, ages, and the tissue site with the maximum frequency (where applicable) are indicated. Multimer combinations chosen based on donor HLA type are indicated. Representative flow cytometry for CMV-seronegative controls are for donor 177 (blood), donor 200 (BM), donor 105 (spleen), and donor 212 (LLN) with CMV-multimer A2 pp65-NLV, representative of 17 CMV-seronegative donors. (B) Representative flow cytometry plots of CMV-multimer B7 pp65-TPR

Compiling data from all of the donors reveals the intraindividual trends in maximum frequency, but also enables comparison of frequencies in different sites between donors, revealing the highest frequencies in blood and LN, followed by BM and lungs (Fig. 1 D). We further compared CMV-specific CD8$^+$ T cells in tonsils (when available), as sites of primary CMV infection and found that most donors had low frequency multimer$^+$ CD8$^+$ T cells in these sites, independent of their frequency in other sites (Fig. 1 D). Together, these results demonstrate a broad distribution of CMV-specific T cells in tissues, with variations in frequency distribution within and between individuals.

Subset delineation of CMV–specific CD8$^+$ T cells in different anatomical sites

We asked whether the distinct frequency distribution patterns of CMV-specific CD8$^+$ T cells between individuals was a function of their subset. We previously showed that each human tissue compartment (circulation, lymphoid, and mucosal) contained a specific complement of T cell subsets defined by cell surface expression of the CD45RA isoform and CCR7 chemokine receptor into naive (CD45RA$^+$CCR7$^+$), central memory (TCM; CD45RA$^-$CCR7$^+$), effector memory (TEM; CD45RA$^-$CCR7$^-$) and terminally differentiated effector (TEMRA; CD45RA$^+$CCR7$^-$) CD8$^+$ T cells (Thome et al., 2014). Representative profiles of CD45RA/CCR7 expression by CMV-specific T cells in multiple tissues (Fig. 2 A) and individual subset frequency in each site from 20 donors depicted as a heat map (Fig. 2 B) shows that the majority of CMV-specific CD8$^+$ T cells persisted as TEM or TEMRA cells, with some naive-phenotype cells, whereas very few persisted as TCM-phenotype cells. Although there was not a significant correlation between subset frequency and tissue distribution pattern or subset frequency and age (unpublished data), certain trends were noted. For example, in donors with highest frequency in blood or BM, CMV-specific T cells were largely TEM cells in most sites including spleen, LNs, lung, and colon, and TEMRA cells in the blood and lung (Fig. 2, A and B). In certain donors, we also detected significant frequencies of CD45RA$^+$CCR7$^+$ phenotype cells (typically associated with naive T cells) in blood and LNs of donors with higher frequencies in BM, and in LNs of donors with highest frequencies in LNs and those with low frequency

populations in multiple sites (Fig. 2, A and B). These results indicate that donors with large populations of CMV-specific T cells in blood, BM, spleen, and/or lung maintain them as TEMRA and TEM cells, whereas donors with large LN or low frequency populations maintain virus-reactive T cells both as TEM and CD45RA$^+$CCR7$^+$ subsets.

CMV–specific CD8$^+$ cells in blood, BM, spleen, and lung exhibit profiles of previous activation

We examined whether the activation and functional state of CMV-specific CD8$^+$ T cells in blood and tissues differed in donors with distinct tissue distribution patterns. As TEM in tissues are subject to tissue-specific influences (Thome et al., 2014), we examined whether CMV-specific CD8$^+$ T cells in tissues exhibited phenotypes of tissue residence based on CD69 expression as a marker of TRM cells (Thome et al., 2014), previous activation, and proliferation based on CD28 expression (Vallejo et al., 1999) and replicative senescence by CD57 expression (Di Benedetto et al., 2015). For each parameter in each site, we compared the profile of CMV multimer$^+$ (CMV-specific) and CMV multimer–negative (neg., polyclonal) TEM cells, to assess whether the properties of CMV-specific T cells in each site were a function of TEM in that specific site or were specific to the CMV-specific population.

In the donors with highest frequencies of CMV-specific T cells in blood or BM, CD69 expression by CMV-multimer$^+$ CD8$^+$ T cells was similar to the multimer–neg. TEM population in each site. Thus, CMV-multimer$^+$ T cells in blood were uniformly CD69-negative, but in tissue sites they exhibited CD69 up-regulation consistent with the endogenous TEM in each site (27–35% CD69$^+$ in BM and spleen and 34–54% CD69$^+$ in lung and LLN; Fig. 3, A and B). The activation state of CMV-specific CD8$^+$ T cells in blood, BM, spleen, and lung, however, was distinct from polyclonal TEM cells in those sites, based on expression of CD28 and CD57 (Fig. 3, A and B). CMV-multimer$^+$ TEM cells exhibited reduced CD28 expression and increased CD57 expression compared with CMV-multimer–neg TEM cells in blood, spleen, LLN, and lung (Fig. 3, A and B), indicative of increased activation and replicative senescence (Vallejo et al., 1999; Di Benedetto et al., 2015). CMV-specific CD8$^+$ T cells in these active sites (blood, BM, spleen, and lung) were functionally robust, exhibiting higher perforin expression compared with TEM cells

---

staining of live CD3$^+$CD19$^-$CD4$^-$CD8$^+$ cells (left) and IFN-γ secretion and CD69 expression of live CD3$^+$CD4$^-$CD8$^+$ after 6-h culture without peptide (unstim) or with CMV peptide mixes for pp65 and IE-1 (right; see Materials and methods) from blood of a 73-yr-old male (D262). (C) Individualized CMV-multimer frequency results for 20 donors showing four distinct distribution patterns: Highest frequency of CMV-multimer$^+$CD8$^+$ T cells in blood compared with other sites (Blood > all; red lines; four donors); highest frequency in BM compared with other sites (BM > all; black lines; nine donors); highest frequency of in LNs compared with other sites (LN > all, blue lines, three donors); and low frequency throughout multiple sites (green lines; four donors). Each line represents one donor, with each donor having a unique symbol. Individual CMV multimer$^+$ frequencies and usage are shown in Table 2. (D) Compiled results showing mean frequency (±SEM) of CMV-specific T cells from multiple donors stratified into four distribution patterns of CMV-multimer$^+$CD8$^+$ T cells in blood and tissues: Blood > all (n = 4; red); BM > all (n = 9; black); LN > all (n = 3; blue); and low frequency in all tissue sites (n = 4; green). The mean (±SEM) number of CMV-multimer$^+$ T cells detected in each sample was as follows: blood, 577 (±301); BM, 2,552 (±837); spleen, 1,470 (±340); LLN, 1,349 (±727); MLN, 2,254 (±1,350); ILN, 712 (±306); lung, 964 (±223); colon, 168 (±71); and tonsils, 715 (±595). Flow cytometry staining for each donor was performed in triplicate. Numbers in the flow cytometry plots indicate the percent of cells expressing given markers.

in LN (Fig. 3, A and B). We also measured IFN-γ production by CMV-multimer⁺ T cells after short-term stimulation with PMA/ionomycin, which preserved CMV-multimer staining (Fig. 3 C). After stimulation, IFN-γ production by CMV-specific and polyclonal TEM cells was higher in lymphoid tissue compared with blood, spleen, and lung (Fig. 3, D and E). Together, these results demonstrate that blood, BM, spleen, and lung may be sites of previous CMV-specific T cell activation, particularly in donors with high relative frequencies of CMV-specific T cells in blood or BM.

Table 2. Frequency of CMV-multimer⁺ CD8⁺ T cells in tissues of individual donors as assessed by staining with individual or combinations of multimer reagents

Donor	Age	CMV-multimer	CMV-multimer⁺ CD8⁺ T cell frequency					Tissue with max. Freq.
			Blood	BM	Spleen	LLN	Lung	
	yr		%	%	%	%	%	
201	21	B7 pp65-RPH + B7 pp65-TPR	1.3	6.7	1.0	0.8	3.4	BM
		B7 pp65-RPH	0.47	1.96	0.28	0.36	1.03	
		B7 pp65-TPR	1.03	6.14	0.87	0.8	3.00	
146	23	A2 pp65-NLV	2.3	11.3		1.9	4.1	BM
207	23	A2 IE1-VLA + A2 IE1-VLE	1.2	1.5	1.3	0.3		None/low
		A2 IE1-VLA		0.35	0.08	0.04		
		A2 IE1-VLE		0.85	1.12	0.28		
103	25	A2 pp65-NLV	12.7	2.2	1.0	0.6	1.5	Blood
227	26	A3 IE1-KLG	0.1	0.9	0.1	2.0	0.1	None/low
169	33	A3 IE1-KLG + A24 pp65-QYD + A24 pp65-VYA	0.5			12.7	2.7	LN
216	34	A2 pp65-NLV + A2 IE1-VLA + A2 IE1-VLE	0.7	0.4	0.9	0.4	0.9	None/low
		A2 pp65-NLV			0.34	0.49	0.61	
		A2 IE1-VLA			0.19	0.37	0.86	
		A2 IE1-VLE			0.40	0.36	0.75	
174	35	B7 pp65-RPH + B7pp65-TPR	3.4	5.4	4.4	2.1	4.6	BM
		B7 pp65-RPH	1.91	2.35	1.87		1.51	
		B7 pp65-TPR	5.8	4.60	3.37		3.02	
147	36	A2 pp65-NLV + A24 pp65-QYD	1.0	8.5	4.2	2.5	0.2	BM
		A2 pp65-NLV		8.33	1.75			
		A24 pp65-QYD		2.50	0.44			
150	39	A24 pp65-QYD	0.2	0.1	3.9	12.1	3.9	LN
156	40	A2 pp65-NLV	1.6	2.1		0.6		LN
196	45	A2 pp65-NLV + A2 IE1-VLA + A2 IE1-VLE	4.0	8.5		1.6	3.5	BM
172	49	B7 pp65-RPH + B7pp65-TPR	2.2		2.0	1.3	3.9	BM
		B7 pp65-RPH			0.80		1.00	
		B7 pp65-TPR			0.59		1.56	
217	49	B7 pp65-RPH + B7pp65-TPR	24.6	10.4	4.4	0.7	5.4	Blood
		B7 pp65-RPH		4.62	1.01	0.26	1.24	
		B7 pp65-TPR		4.76	1.87	0.37	4.80	
199	50	A2 pp65-NLV + A2 IE1-VLA + A2 IE1-VLE + A3 IE1-KLG	10.1	NA	4.4	0.6	5.5	Blood
		A2 pp65-NLV	1.24		0.71	0.18	0.38	
		A2 IE1-VLA	6.35		3.61	0.44	3.79	
		A2 IE1-VLE			0.07			
		A3 IE1-KLG	2.35		0.11	0.55	1.20	
194	53	A24 pp65-QYD + B7 pp65-TPR	0.2	3.6	1.2	0.6	1.0	BM
		A24 pp65-QYD	0.2	1.9	1.2	1.2	1.85	
		B7 pp65-TPR	0.11	2.94	0.46	0.09	0.20	
208	54	A3 IE1-KLG + B7 pp65-RPH + B7 pp65-TPR	3.7	7.6	5.1	1.2	2.5	BM
		A3 IE1-KLG	0.21	1.53	1.80	0.33	0.88	
		B7 pp65-RPH	3.08	7.41	3.97	1.32	1.88	
		B7 pp65-TPR	0.74	1.36	1.23	0.33	0.28	
220	64	A2 pp65-NLV + A24 pp65-QYD	0.3	0.6	0.5	0.9	0.5	None/Low
		A2 pp65-NLV	1.38	0.32	0.9	0.8	0.6	
		A24 pp65-QYD	0.36	0.05	1.24	1.21	0.05	
226	66	A1 pp50-VTE + A1 pp65-YSE	31.6	5.4	0.9	1.9	3.1	Blood
		A1 pp50-VTE		0.08	0.08	2.7	0.06	
		A1 pp65-YSE		5.6	0.9	4.0	3.3	
197	70	A1 pp50-VTE + A1 pp65-YSE	NA	NA	NA	5.4	8.2	NA

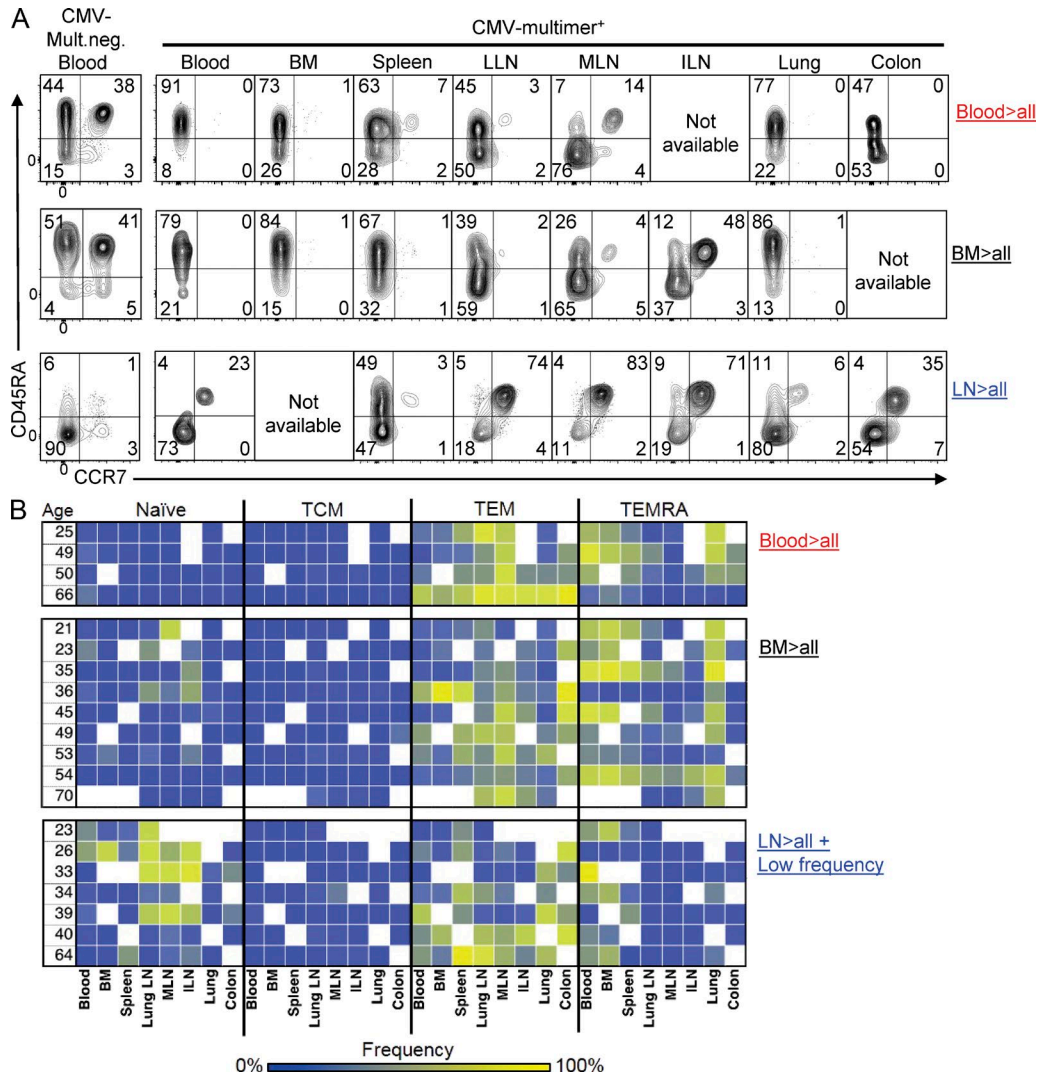Only 61 CD8⁺ T cells with CMV multimer frequency of 4.9%.

Figure 2. **Subset delineation of CMV–specific CD8+ T cells in donors with distinct tissue distribution patterns.** Subset delineation of CMV-specific CD8+ T cells in each site was defined based on CD45RA and CCR7 expression. (A) Flow cytometry plots of CD45RA and CCR7 expression delineates four major subsets in each quadrant: naive (CD45RA+CCR7+, top right), TCM (CD45RA−CCR7+, bottom right), TEM (CD45RA−CCR7−, bottom left), and TEM RA (CD45RA+CCR7−, top left), in eight tissue sites. (left) Representative gating for CD45RA and CCR7 for CMV-multimer neg. cells from blood of each donor. (right) Coordinate expression of CD45RA and CCR7 gated on CMV-multimer+CD3+CD19−CD4−CD8+ T cells from donors with highest frequencies of CMV-specific T cells in blood (donor 217, 49 yr old; top row), BM (donor 174, 35 yr old; middle row), and LN (donor 150, 39 yr old; bottom row). CMV-multimers used for each donor are indicated in Table 2. (B) Heat map of CMV-specific CD8+ naive, TCM, TEM, and TEMRA cell frequency (ranging from 0% [blue] to 100%, [yellow]) based on the gating in A in 20 individual donors stratified by frequency distribution pattern of CMV-specific cells identified in Fig. 1 and ranked according to age. Flow cytometry staining for each donor was performed in triplicate panels. Numbers in the flow cytometry plots indicate the percent of cells expressing given markers.

We also assessed the activation and functional state of CD45RA+CCR7+ CMV-specific T cells that were found in some of the donors with high frequencies in blood and BM (Fig. 2, A and B). Although polyclonal CD45RA+CCR7+ T cells in blood and lymphoid tissues were CD28+/CD57− (Fig. 3, F and G), which is consistent with this subset being naive T cells, CMV-specific CD45RA+CCR7+ cells exhibited significantly decreased CD28 and increased CD57 expression in BM, spleen, and lung, suggesting previous

activation in these sites. After stimulation, significant proportions of CMV-specific CD45RA+CCR7+ cells produced IFN-γ and expressed CD107a, a marker of cytotoxic granulation (Betts et al., 2003) in blood, BM, lymphoid tissues, and lungs, whereas polyclonal naive cells in these sites did not produce these effector molecules (Fig. 3, F and G). These CMV-specific CD45RA+CCR7+ cells in donors with high frequency populations in the blood or BM therefore exhibit features of activated or memory T cells. Together, these results
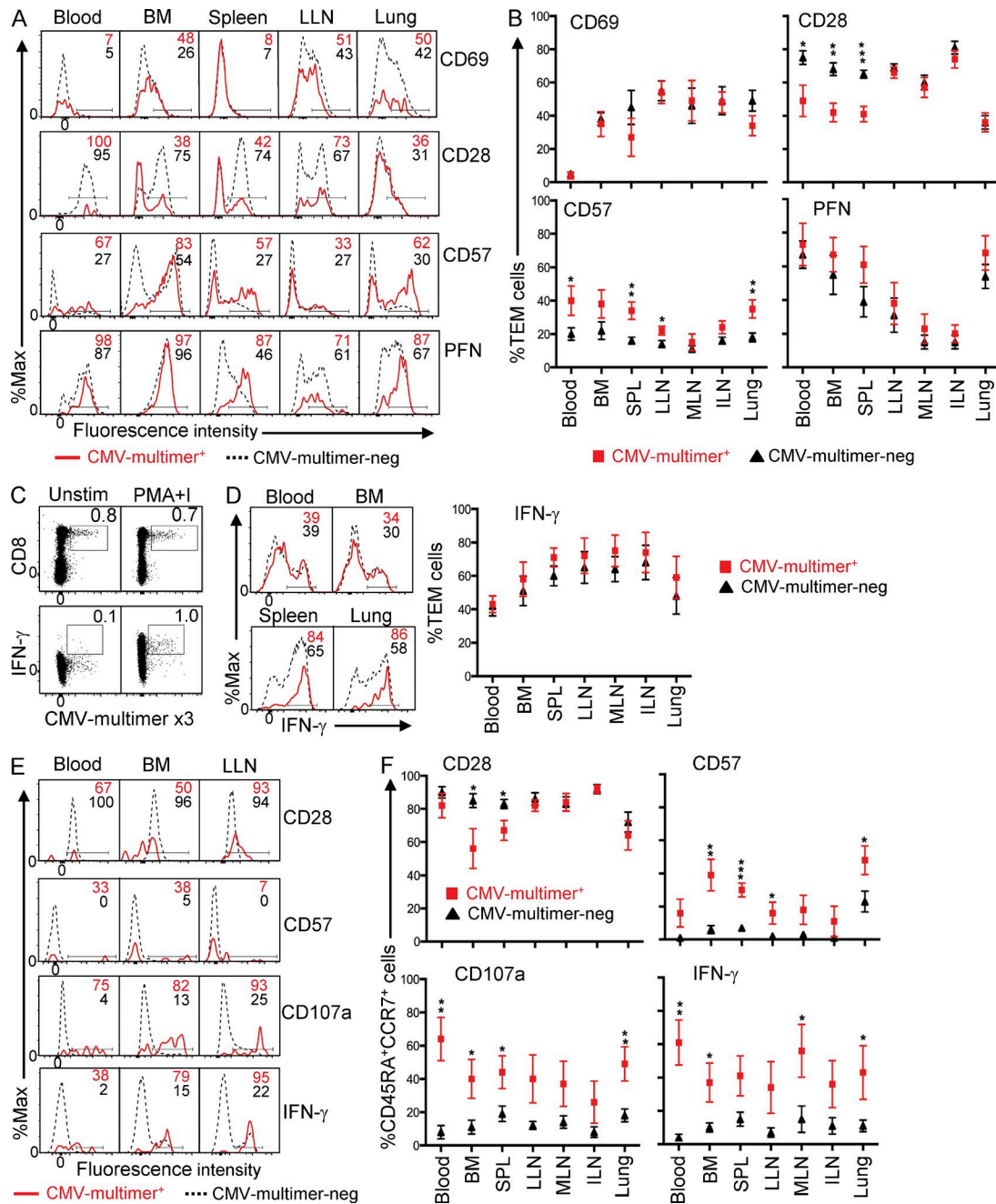
Figure 3. CMV-specific T cells in donors with the highest frequencies in blood or BM exhibit phenotypes of previous activation. The phenotype and function of CMV-specific T cells from donors with the highest frequencies in blood and BM were examined (*n* = 13 total). (A) Expression of cell surface markers (CD69, CD28, and CD57) and intracellular perforin (PFN) by CMV-multimer⁺ TEM CD8⁺ T cells (solid red) compared with CMV-multimer–negative (-neg.) TEM CD8⁺ T cells (dotted black) in blood, BM, spleen, LLN, and lung. Shown are representative histograms of CD69 (donor 147, top row), CD28 (donor 194, second row), CD57 (donor 201, third row), and PFN (donor 201, fourth row) expression by TEM cells stained directly ex vivo. (B) Mean frequency (±SEM) of CMV-multimer⁺ (red squares) and CMV-neg. (black triangles) CD8⁺ TEM cells expressing markers as in A in blood and indicated tissues, compiled from 13 donors. Number of donors for each graph was as follows: CD69 (*n* = 5–9 per site), CD28 (*n* = 8–10 per site), CD57 (*n* = 8–11 per site), and PFN (*n* = 6–7 per site). (C) Representative flow cytometry plots of CMV-multimer staining of live T cells (top row) and IFN-γ production by CMV-multimer⁺ CD8⁺ T cells (bottom row) after 3-h culture without stimulation (Unstim.) or with PMA/ionomycin (PMA + I). (D; left) IFN-γ production by CMV-multimer⁺ TEM CD8⁺ T cells (red) compared with CMV-neg. TEM CD8⁺ T cells (black) in blood, BM, spleen, and lung of donor 217 by intracellular cytokine staining after stimulation with PMA/ionomycin (see Materials and methods). (right) Mean frequency (±SEM) of CMV-multimer⁺ (red squares) and CMV-multimer-neg. (black triangles) CD8⁺ TEM cells producing IFN-γ in blood and indicated tissues, compiled from eight donors (*n* = 4–8 per site). (E) Expression of cell surface markers (CD28 and CD57), and CD107a expression and IFN-γ production by CMV-multimer⁺ CD45RA⁺CCR7⁺ CD8⁺ T cells (solid red) compared with CMV-multimer-neg.

provide evidence of a dynamic T cell response within tissues of individuals containing high frequencies CMV-specific T cells in the blood or BM.

Donors with high frequencies in LN or low frequency distribution have quiescent CMV-specific T cells

CMV-specific TEM cells from donors with high frequencies in LN or low frequencies in many sites did not exhibit features of previous activation, as they were largely CD28^{+} and CD57^{−}, similar to CMV-multimer–neg. TEM cells in the corresponding tissue site (unpublished data). CMV-specific CD45RA^{+}CCR7^{+} cells in LNs were likewise similar to polyclonal naive T cells, exhibiting CD28^{+}/CD57^{−} phenotypes indicative of resting T cells, and did not produce IFN-γ, IL-2, or degranulate (as measured by CD107a) after stimulation (Fig. 4, A and B; and not depicted). Together, this analysis indicates that CMV-specific CD8^{+} T cells persist in a quiescent state in donors with predominant frequencies in LN, or with low frequencies throughout.

The extent of multimer binding to the TCR, as estimated by the mean fluorescent intensity (MFI), correlates with TCR avidity (Laugel et al., 2007) and may indicate recent antigen–driven expansion. As another measure of activation or quiescence, we examined multimer binding profiles of CMV-specific T cell subsets in different sites of donors with highest frequencies in BM or LN. In a representative donor with high frequencies in BM, CMV-specific TEM and TEM RA cells exhibited a higher MFI of multimer binding compared with CMV-specific CD45RA^{+}CCR7^{+} cells from the same site (Fig. 4 C). In contrast, in donors with high frequencies in LN, both TEM and CD45RA^{+}CCR7^{+} CMV-specific populations exhibited a low MFI of multimer binding in tissues (Fig. 4 C). These results provide additional evidence that CMV-specific CD8^{+} T cells in donors with biased maintenance in BM and blood exhibit phenotypes indicative of previous activation while those maintained in LN or at low levels in many sites exhibit features suggestive of a quiescent state.

To test whether the CMV-specific CD8^{+} T cells with low TCR binding avidity were able to respond to CMV-specific epitopes, we stimulated low multimer-binding CD8^{+} T cells from BM, spleen and LLN with CMV-pp65 peptides and analyzed the resultant expanded population. We found significant activation and expansion of CMV-specific T cells from each site, particularly with spleen and LLN-derived T cells, and CMV-multimer binding of the pp65-expanded population was augmented 19-fold as assessed by MFI

(Fig. 4 D). These results demonstrate that the low avidity CMV-specific T cell populations are fully responsive to CMV antigen, and that higher avidity populations observed in BM, blood, and lungs may indicate previous or recent activation.

CMV persistence in circulation and tissues inversely correlates to the T cell response

We hypothesized that the tissue distribution and/or activation state of CMV-specific CD8^{+} T cells may be influenced by the presence of virus in these sites. The precise reservoir of CMV is not known, although CMV latency has been described in human BM CD34^{+} hematopoietic progenitors, circulating CD14^{+} monocytes, dendritic cells, and alveolar macrophages (Hahn et al., 1998; Reeves and Sinclair, 2013; Poole et al., 2015). The persistence of CMV genomes in mononuclear cells from seropositive individuals is also quite rare, representing 1/10,000 cells, as observed in a previous study (Slobedman and Mocarski, 1999). We assessed the presence of CMV genomes in total mononuclear cells obtained from donor blood and tissues using a highly sensitive quantitative PCR approach that we developed and optimized specifically to detect CMV gene targets conserved between multiple clinical strains (see Materials and methods). CMV genome analysis was performed on 123 samples from 10 tissues sites of 24 CMV-seropositive (Fig. 5) and –seronegative donors.

CMV genomes were detected in 76% (16/21) of CMV seropositive donors, whereas there were no detectable CMV genomes in tissues from CMV-seronegative donors (Fig. 5 A and not depicted). In all cases, detection of CMV genomes was at or near the level of detection, consistent with the low level of CMV persistence that is a feature of its latency (Goodrum, 2016). The frequency of CMV detection varied as a function of tissue site, with lung having the highest frequency of CMV detected (61% 11/18), followed by LNs (29–37%); blood, spleen, and BM had lower overall frequencies of CMV detection (13–25%; Fig. 5 A). Examination of the individual CMV detection data for each donor (Table 3) reveals that the majority of donors (12/21) had CMV detected in more than one tissue site, with 4/21 donors having CMV detected in one site (primarily the lung); in 5/21 donors, CMV was not detected in any of the sites analyzed. There was no overall correlation between the pattern of CMV detection in tissues and the distribution pattern of CMV-specific CD8 T cells (Table 3). However, CMV genomes were rarely detected in the blood and BM of donors with high frequencies of CMV-specific T cells in these sites, whereas CMV genomes

---

CD45RA^{+}CCR7^{+} CD8^{+} T cells (dotted black) in blood, BM, and LLN from the same donors as in A. Surface CD107a and intracellular IFN-γ production was measured after stimulation with PMA/ionomycin. Shown are histograms of CD28 (first row), CD57 (second row), CD107a (third row), and IFN-γ (fourth row) of indicated subsets from donor 196, analyzed as in A. (F) Mean frequency (±SEM) of CMV-multimer^{+} (red squares) and -neg. (black triangles) CD45RA^{+}CCR7^{+} CD8^{+} T cells expressing CD28, CD57, CD107a, and IFN-γ in blood and indicated tissues, compiled from 13 donors. Number of donors for each graph: CD28 (n = 8–10 per site), CD57 (n = 8–11 per site), CD107a (n = 5–8 per site), and IFN-γ (n = 4–8 per site). Significant differences for comparison of means between CMV-multimer^{+} and -neg. CD8^{+} T cells within each tissue site were determined by Student's t test and corrected by Holm-Sidak for multiple comparisons. *, P = 0.05–0.011; **, P = 0.01–0. 001; ***, P < 0.001. Numbers in the flow cytometry plots indicate the percent of cells expressing given markers.
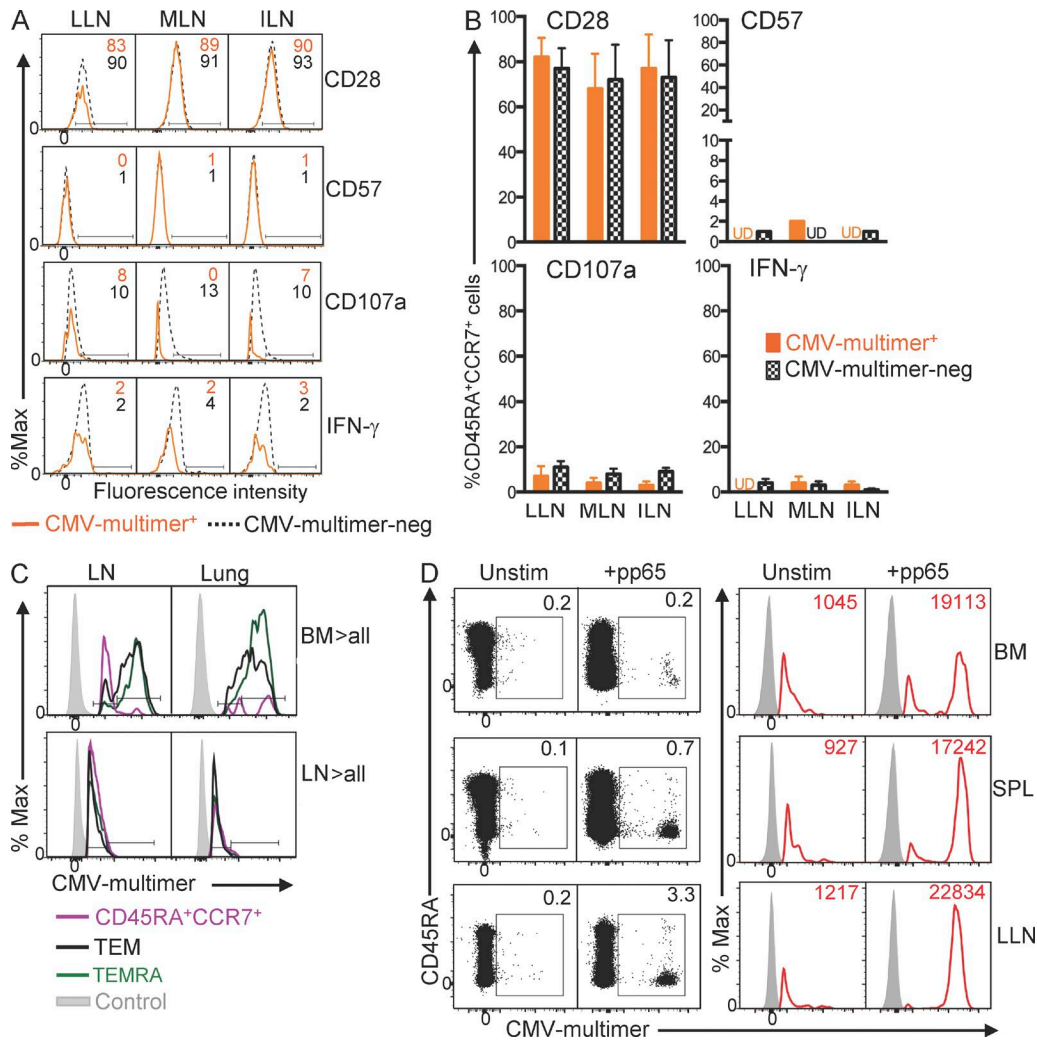
Figure 4. CMV–specific T cells are quiescent in donors with highest frequencies in LN or low frequency distribution patterns. (A) Phenotypic and functional properties of CMV-specific CD45RA+CCR7+CD8+ T cells in LNs from donors with the highest frequencies in LN or low frequencies in multiple sites (seven donors total). Shown are histograms of CD28 (donor 169, first row), CD57 (donor 169, second row), CD107a (donor 207, third row), and IFN-γ (donor 207, fourth row) in CMV-multimer+ (solid orange line) compared with CMV-multimer-neg. (dotted black line) CD45RA+CCR7+CD8+ T cells. (B) Graphs show expression of surface and functional markers as mean frequency (±SEM where appropriate) of CD28+, CD57+, CD107a, and IFN-γ+ CMV-multimer+ (orange bars) compared with -neg CD45RA+CCR7+CD8+ T cells (checkered black) in LLN, MLN, and ILN. Significant differences for comparison of means between CMV-multimer+ and -neg. CD45RA+CCR7+CD8+ T cells within each tissue site were determined by Student's t test and corrected by Holm-Sidak for multiple comparisons, with no significant difference found within a given site. Number of donors for each graph: CD28 (n = 4–6 per site), CD57 (n = 2–4 per site), and IFN-γ (n = 3–5 per site). (C) CMV-specific CD8+ T cells vary in multimer avidity as a function of tissue and distribution pattern. Representative histograms of CMV-multimer fluorescence intensity by CD45RA+CCR7+ (violet), TEM (black), and TEMRA (green) subsets in LN and lung compared with the CMV-multimer-neg. control (shaded gray) from a donor with highest frequencies in BM (top row, donor 201) and a donor with highest frequencies in LN (bottom row, donor 150). (D) Increased multimer avidity of CMV-specific T cells after CMV peptide stimulation. Total mononuclear cells from BM, spleen and LLN (donor 194) were stimulated for 9 d with pp65 peptide mix (see methods). Left: Frequency of CMV-multimer+ CD8+ T cells before and after stimulation. (right) CMV-multimer staining in unstimulated versus pp65-expanded CD8+ T cells, with numbers in plots denoting MFI of CMV-multimer staining. Cells were pooled from triplicate samples. Numbers in the flow cytometry plots indicate the percent of cells expressing given markers.

were variably detected in multiple tissues of donors maintaining CMV-specific T cells in LNs, or at low or undetectable frequencies throughout multiple sites (Fig. 5 B). Of note, individuals with high frequency CMV-specific T cells in circulation (blood and BM), had no detectable CMV genomes in these sites (Fig. 5 B). In contrast, in the spleen, LLN, and lung,

the frequency of CMV-specific T cells was similar whether or not CMV genomes were detected (Fig. 5 B). Together, these results suggest a site-specific interaction between T cells and virus with no detectable virus in circulating sites with high T cell frequencies and equilibrium between the virus and T cells in lung and LN reservoirs.
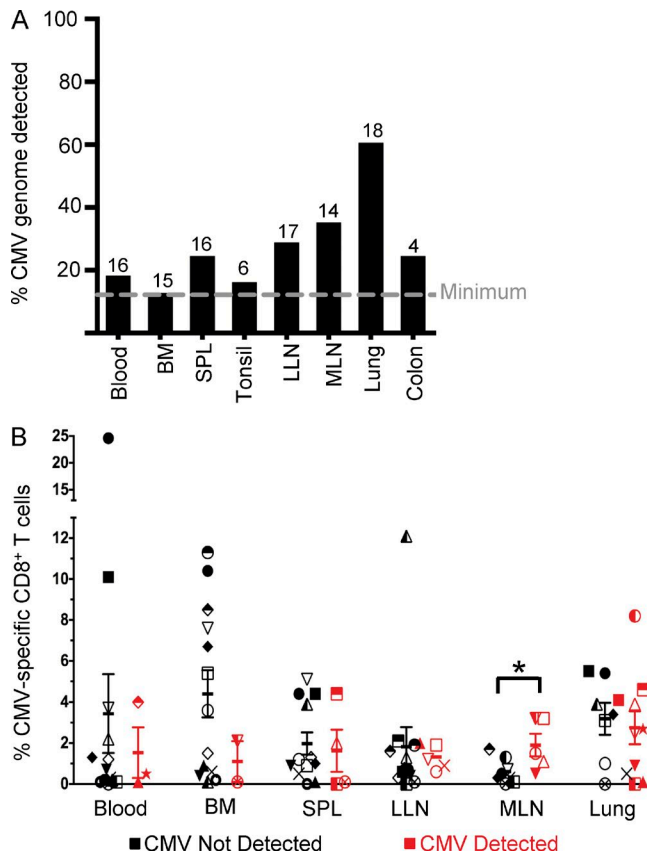
Figure 5. **CMV persistence and CMV–specific T cell responses in circulation and tissues.** (A) Mean frequency of detection of CMV genomes in tissues of 21 CMV-seropositive donors. Dashed gray line indicates the minimum frequency of CMV genome detection for all tissue sites. Numbers above the bars represent the number of samples tested for each tissue. Each sample was run in 10–13 replicates and scored as "detected" (CMV genome targets detected in any replicate) or not detected (no CMV genome targets detected in any replicate). (B) Mean frequency (±SEM) of CMV-specific T cells in tissues of donors in which CMV genomes were detected (red) or not detected (black), compiled from 18 donors. Each shape denotes an individual donor. Significant differences for comparison of means between donors in which CMV genomes were detected (red) or not detected (black) within each tissue site were determined by Student's *t* test and corrected Holm-Sidak for multiple comparisons. *, P < 0.05, and no significant differences found for other sites.

Overall impact of CMV infection on T cell differentiation in circulation and tissue sites over age

Given the preferential persistence of CMV-specific T cells in distinct sites and reported influence of CMV persistence on overall T cell differentiation and immune function (Chidrawar et al., 2009), we investigated potential effects of CMV infection on T cell differentiation in tissues. We took advantage of our accumulated analysis of T cell subsets in tissue sites of over 72 donors and compared CD8$^+$ T cell subset distribution in 10 tissue sites from 44 CMV-seropositive and 28 CMV-seronegative organ donors of similar age ranges (14–75 yr; Fig. 6 A and Table S2). Compiled results reveal decreased

frequency of naive CD8$^+$ T cells starting in young adulthood in CMV seropositive donors compared with CMV seronegative donors in blood, BM, LLN, and lung, which declines further over decades (Fig. 6 B, first row). Conversely, there is an increased frequency of TEMRA CD8$^+$ T cells in blood, BM, spleen and lung, and an increase in the TEM CD8$^+$ T cells in the LLN in CMV seropositive compared with seronegative donors, which further increases with age. Together, these results indicate enhanced T cell differentiation in specific sites of CMV seropositive donors. A similar decrease in the proportion of naive CD4$^+$ T cells with a concomitant increase in proportion of CD4$^+$ TEM over life in blood, BM, LLN, and lung was observed in CMV seropositive compared with seronegative donors (Fig. 7). We also observed an increase in CD4$^+$ TEMRA cells specifically in the BM, a population previously described in the blood and BM of CMV seropositive individuals (Libri et al., 2011). These data demonstrate that CMV infection exerts a global influence on T cell homeostasis that extends beyond the circulation to the tissues.

DISCUSSION

Our knowledge of T cell immunity to persistent viruses in humans has mostly been limited to analysis of peripheral blood. Using our novel human organ donor tissue resource, we investigated antiviral T cell immunity and viral persistence in the circulation and diverse tissues during a dynamic and persistent viral infection, CMV. Our analysis reveals individualized patterns of tissue T cell anti-CMV immunity and insights into how tissue location impacts antiviral T cell responses. We identify potential sites of active T cell–mediated viral clearance (blood, BM, and spleen), and reservoirs of viral persistence coexisting with either an active (lung) or quiescent (LN) T cell response. Furthermore, CMV persistence exerts global effects on T cell homeostasis in a tissue-dependent manner. Overall, our results reveal how CMV-specific T cells are distributed and function in multiple sites in the context of tissue location and viral persistence, providing new insights into immune control of CMV infection in the body.

Our results show that the frequency of CMV-specific CD8$^+$ T cells in tissues invariably differs from that in blood. Previous studies comparing CMV-specific T cells in peripheral blood to an additional site (either BM, LN, tonsils or lung) also found discordance in blood and tissue frequencies, with tissue responses less frequent than blood in the individuals examined (de Bree et al., 2005; Letsch et al., 2007; Sauce et al., 2007; Palendira et al., 2008; Remmerswaal et al., 2012; Akulian et al., 2013). By examining a broader array of tissues from each individual compared with what has previously been examined, we found the highest frequency of CMV-specific T cells to be in blood compared with other sites in a subset of donors; however, the majority of the donors had biased high frequencies in BM or LN, or comparable low frequencies throughout all sites. There are several possibilities that could contribute to differential persistence of blood-versus-tissue CMV-specific responses; either blood
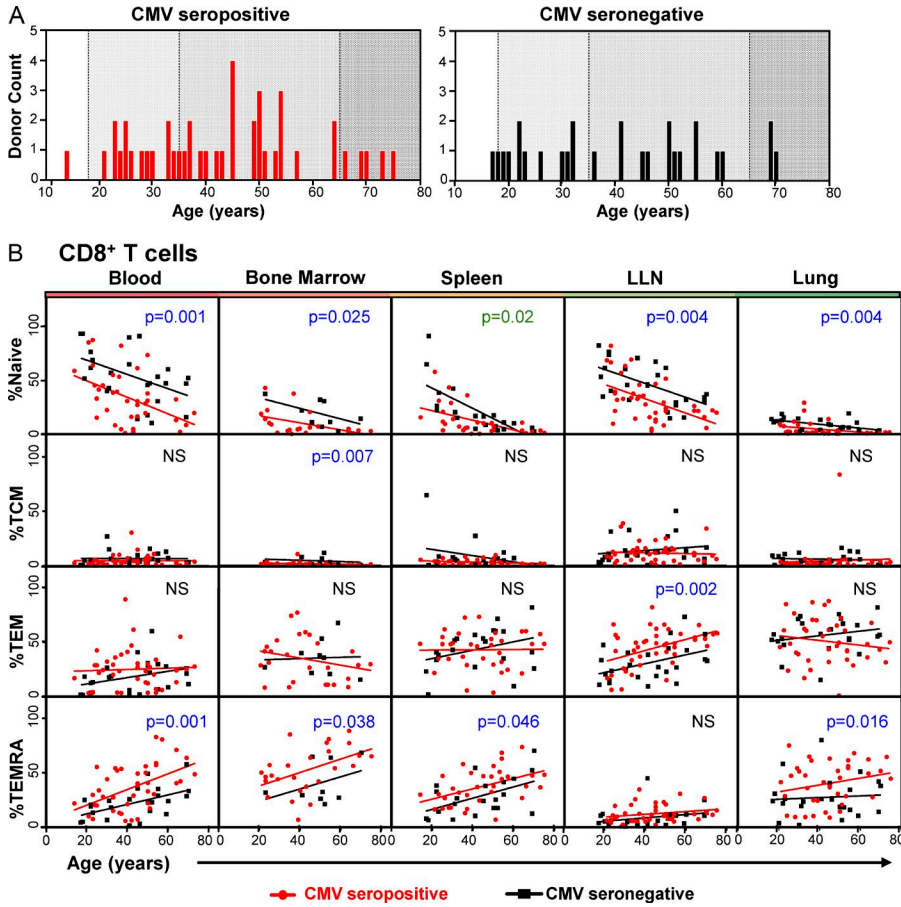
Figure 6. **CMV infection has global effects on tissue CD8+ T cell differentiation and homeostasis.** (A) Age distribution of CMV-seropositive (red, n = 44) and CMV-seronegative (black, n = 28) donors divided into four age groups: Youth (<18 yr, white), young adult (18–35 yr, light gray), adult (36–65 yr, gray), and senior (≥66 yr, dark gray). Donor information shown in Table S3. (B) Graphs show total CD8+ T cell subset distribution based on overall phenotype (naive, TCM, TEM, and TEM RA, based on CD45RA/CCR7 expression) in the indicated tissues from CMV-seropositive (red lines) and -seronegative (black lines) donors as a function of age, with each dot representing an individual donor and changes with age determined by linear regression analysis. Significant P-values for comparison of slope regression lines between seropositive and -negative are shown in green; P-values for the comparison of slope intercepts are shown in blue and nonsignificant P-values for the comparison of slope intercepts are denoted by NS.

Table 3. **CMV PCR analysis of tissues from individual donors compared to the tissue–distribution pattern of CMV–specific CD8+ T cells**

Age	Blood	BM	Spleen	LLN	MLN	Lung	Other	Tissue site with max. freq.
yr								
21	−	−	−	−	−	−	Tons−	BM
23	n/a	−	n/a	−	n/a	+		BM
35	n/a	n/a	+	−	n/a	+	ILN+	BM
45	+	−	n/a	−	−	n/a		BM
49	−	n/a	+	−	+	+	Col+, Tons−	BM
49	−	−	−	−	−	−		Blood
50	−	n/a	−	−	n/a	−		Blood
53	−	−	−	+	+	−	Tons−	BM
54	−	−	−	+	−	+	ILN−, Col−	BM
66	n/a	−	−	+	+	−		Blood
70	n/a	n/a	n/a	n/a	−	+		BM
23	−	−	−	−	−	+	ILN−	Low
26	+	−	−	+	n/a	+	Tons−	Low
30	−	n/a	+	−	−	+		None
33	+	n/a	n/a	n/a	n/a	+	Tons+	LN
34	−	−	−	−	+	+	Col−	Low
37	−	+	+	−	−	−		None
39	−	−	−	−	n/a	−	Col−	LN
40	n/a	+	n/a	n/a	+	n/a		LN
54	−	−	−	n/a	n/a	n/a		None
64	−	−	−	+	−	+	ILN−, Tons−	Low

+, CMV genome detected; −, CMV genome not detected; Col, Colon; Tons, tonsil; n/a: tissues not available.
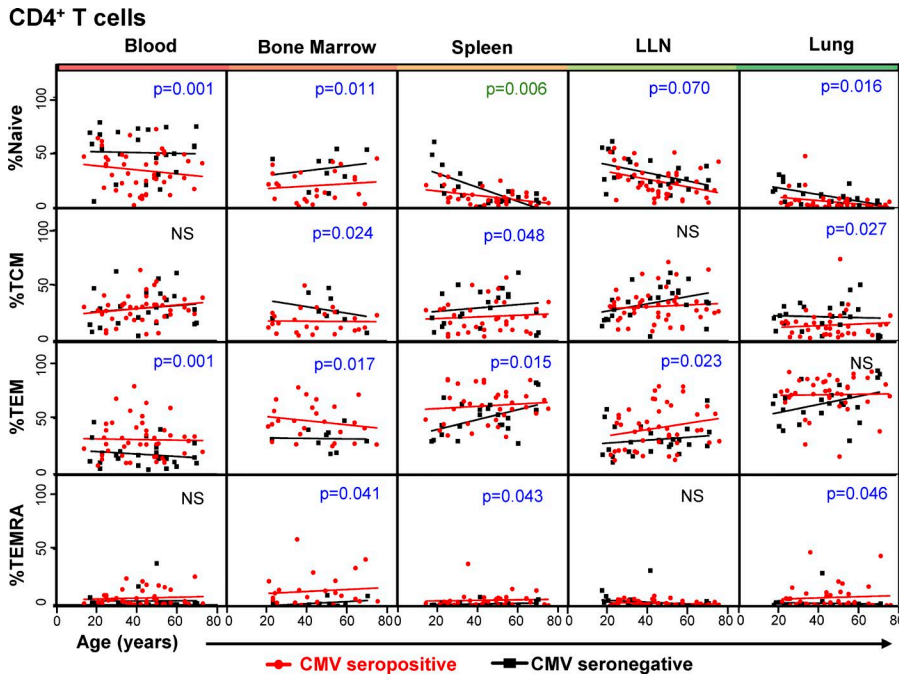
CD4+ T cells

Figure 7. **CMV infection has global effects on tissue CD4+ T cell differentiation and homeostasis.** Graphs show total CD4+ T cell subset distribution based on overall phenotype (naive, TCM, TEM, and TEMRA, based on CD45RA/CCR7 expression) in the indicated tissues from CMV-seropositive (red lines) and -seronegative (black lines) donors as a function of age, with each dot representing an individual donor and changes with age determined by linear regression analysis, as in Fig. 6. Significant p-values for comparison of slope regression lines between seropositive and -negative are shown in green; P-values for the comparison of slope intercepts are shown in blue, and nonsignificant P-values for the comparison of slope intercepts are denoted by NS.

represents its own niche for maintenance of antiviral T cells, certain tissues harbor resident subsets of CMV-specific T cells, and/or dynamic activation events in certain sites leads to differential egress of T cells from tissues into circulation. Notably, individuals with high frequencies of CMV-specific T cells in blood (or BM) maintained these populations as TEM or TEM RA cells bearing features of recent activation and replicative senescence, whereas donors with predominantly CMV-specific T cells in LNs and/or with no significant circulating blood or BM populations were instead maintained as quiescent subsets. These results suggest that blood (and BM) could be a repository for activated T cells generated during a dynamic response to infection, which is consistent with findings of newly activated CD8+ T cells appearing in the blood after vaccination with live viruses (Miller et al., 2008) or during acute influenza infection (Sridhar et al., 2013). Further, in-depth profiling of tissue CMV-specific T cells compared with blood in future studies will enable a more precise definition of how circulating antiviral T cells relate to those in tissues.

We hypothesized that the differential distribution and activation phenotypes of CMV-specific T cells in tissues may be a result of the presence of persistent virus in these sites. We therefore assessed CMV persistence in donor tissues as cellular and tissue reservoirs of CMV latency remain undefined in humans (Goodrum et al., 2012). We identify CMV persistence predominantly in the lung and also in spleen, BM, blood, and LN. The identification of the lung as a potential reservoir of persistent CMV is consistent with recent results showing that CMV is present in alveolar macrophages (Poole et al., 2015) and that CMV reactivation is often manifested clinically as pneumonitis (Ljungman et al., 2010; Santos et al., 2015). Persistence of CMV in multiple sites can also account

for the diverse tissue involvement during CMV reactivation and disease, and the sensitivity of immune-mediated control of CMV to immunosuppression.

Integrating our results on CMV-specific T cell distribution, tissue-specific T cell phenotypes, and CMV persistence provides a new view into the dynamic interplay between the immune response and virus. Importantly, there was an inverse correlation in BM and blood between T cell frequency and CMV detection where the highest T cell frequencies were associated with complete lack of CMV detection. As the majority of CMV-specific T cells in blood and BM of these donors with no virus detected exhibited phenotypic features of previous activation, it is intriguing to speculate that these sites may undergo continual surveillance and viral control. Activated T cell populations are observed in circulation during CMV reactivation in immunosuppressed individuals (Hakki et al., 2003), and it will be interesting to determine whether CMV-specific T cells that emerge in circulation during infection carry a trace of their tissue of origin. CMV-specific CD8+ T cells were consistently present in frequencies of 2–6% of total CD8 T cells in donor lungs, and exhibited an activated phenotype, suggesting that the lung is a consistent site of ongoing CMV-specific immune responses without complete viral clearance. In LNs, the frequency of CMV-specific T cells was similar in sites with or without detectable CMV genomes, and LN CMV-specific T cells mostly exhibited resting quiescent phenotypes. As LNs have infrequent exposure to microbes and a low inflammatory environment, CMV reactivation may be rare in these sites and LNs may serve as the reservoir for long-term resting CMV-specific T cells.

All of the tissues analyzed in this study were obtained from brain dead organ donors who were managed in the

critical care unit before organ and tissue acquisition by surgical teams for lifesaving transplantation and for this study. Although these donors were all previously healthy and immunocompetent, there are reports of CMV reactivation occurring after traumatic injury (Cook and Trgovcich, 2011). We investigated whether cause of death or length of hospitalization were associated with CMV T cell distribution and/or frequency and CMV detection and did not find any correlations (unpublished data; compiled from data in Tables 1 and 2). Moreover, the low level of virus detection is consistent with latent and controlled infection. Based on all of these criteria, our results on CMV-specific T cell response and CMV persistence in organ donor tissues is likely to represent the healthy state of viral control.

We also examined the overall impact of CMV infection on T cell differentiation and maintenance in tissues over the human lifespan in a larger cohort of 72 donors. Our results showed tissue-specific effects of CMV infection on T cell differentiation in the active sites of CMV persistence and CMV-specific T cell responses—namely in the blood, BM, lungs, and lung LNs. The dynamic interplay between virus and T cell responses in these sites could generate a local proinflammatory milieu that nonspecifically primes innate immune responses in tissues. This evidence for enhanced, tissue-specific T cell differentiation could account for the greater responses to pathogens and vaccines identified in CMV-seropositive compared with CMV-seronegative individuals (Pera et al., 2014; Furman et al., 2015).

CMV infection remains a significant cause of morbidity and mortality in immunocompromised populations (Kotton et al., 2013; Adland et al., 2015; Frantzeskaki et al., 2015), including solid organ and hematopoietic transplant recipients, cancer patients receiving chemotherapy, and the elderly. The site-specific nature of CMV immunity and viral persistence highlights the need for new therapies targeting tissue reservoirs of CMV persistence and the development of blood biomarkers that more accurately reflect the integrity of tissue CMV immune control. Moreover, the findings obtained from our assessment of CMV-specific and/or polyclonal T cell subsets, in conjunction with CMV persistence in multiple anatomical sites, have broad implications for improving immune monitoring, vaccines, and immunotherapies, and prompt further investigation of tissue-specific antipathogen responses and their relationship to circulating counterparts.

MATERIALS AND METHODS
Acquisition of human tissues
Human tissues were obtained from deceased (brain dead) organ donors at the time of organ acquisition for lifesaving clinical transplantation through an approved protocol and Material Transfer Agreement (MTA) with LiveOnNY. Organ donors were free of chronic disease and cancer and negative for HIV, hepatitis B, and hepatitis C. Characteristics of organ donors, including their cause of death and hospitalization length of stay are in Table 1. The study does not qualify as human subjects research, as confirmed by the Columbia University Institutional Review Board, as tissue samples were obtained from deceased individuals. Donor HLA type, and CMV and EBV serology were available from all donors.

Lymphocyte isolation from human lymphoid and nonlymphoid tissues
Tissue samples were maintained in cold saline and brought to the laboratory within 2–4 h of procurement from the donor. Samples were rapidly processed using enzymatic and mechanical digestion to obtain lymphocyte populations with high viability as described in detail (Sathaliyawala et al., 2013; Thome et al., 2014, 2016). Lymphocytes were isolated from blood using lymphocyte separation media (CellGro; CellGenix) and ACK lysis buffer as previously described (Sathaliyawala et al., 2013). Lymphocytes were either analyzed immediately or cryopreserved for future analysis.

Detection and analysis of CMV–specific T cells
HLA multimers reagents containing epitopes of CMV (CMV-multimers) were obtained from Proimmune and Immudex; the CMV A6801 tetramer was obtained from the National Institutes of Health tetramer core (see Table S1 for full list). Staining with multimers was done according to the manufacturer's protocols using HLA-A2 Negative Control (Proimmune) or Immudex Negative Controls (see Fig. S1 for gating). Only samples with >500 $CD8^+$ T cells were included in the analysis. The level of detection of CMV-multimer$^+$ $CD8^+$ T cells was 0.1–0.3% of $CD8^+$ T cells. For CMV peptide stimulation, $1–3 \times 10^6$ mononuclear cells from blood or tissues were plated in 96-well tissue culture plates in complete RPMI medium (RPMI-1640 containing 10% fetal calf serum, 100 U/ml penicillin, 100 µg/ml streptomycin, and 2 mM L-glutamine (Sigma-Aldrich) containing 1 µg/ml HCMV pp65 peptide mix and 1 µg/ml HCMV pp65 peptide mix (PepMix HCMV; JPT Peptide Technologies) and incubated at 37°C for 6 h in the presence of BD GolgiStop (monensin). For intracellular staining, surface stained cells were fixed, washed, and resuspended in permeabilization buffer (BD) before staining with anti–IFN-γ.

Flow cytometry analysis
Fluorochrome-conjugated antibodies used for staining are shown in Table S3. For intracellular staining, surface stained cells were fixed, washed, resuspended in permeabilization buffer (eBioscience), and stained with antiperforin antibodies. For T cell stimulation, $1–3 \times 10^6$ mononuclear cells from blood or tissues were plated in 96-well tissue culture plates in complete RPMI medium containing phorbol-12-myristate –13-acetate (PMA; 50 ng/ml), ionomycin (1 mg/ml) and anti–CD107a and incubated at 37°C for 3 h in the presence of BD GolgiStop (monensin). The cells were washed with PBS and surface stained, fixed, and permeabilized as above, before staining with anti–IFN-γ and anti–IL-2 antibodies. For expansion of CMV-specific T cells, $1–3 \times 10^6$ mononu-

clear cells from blood or tissues were plated in 96-well tissue culture plates at 5×10^5/ml in RPMI-1640, 10% FBS, 1 mM sodium pyruvate, 100 U/ml penicillin, 100 µg/ml streptomycin, 2 mM L-glutamine, and 100 µM β-mercaptoethanol in the presence of 0.3 µg/ml HCMV pp65 peptide mix (JPT Peptide Technologies). IL-2 100 U/ml was added on day 2 and cells were analyzed at day 9 after stimulation. Stained cells were acquired on a 6-laser LSRII analytical flow cytometer (BD) in the CCTI flow cytometry core and analyzed using FlowJo software (Tree Star).

CMV serology
Serum CMV IgG avidity and CMV IgM testing were performed by Quest Diagnostics.

Detection of CMV genomes
Cells were thawed in IMDM with 2% FBS, counted with Trypan blue, and pelleted. Cells were lysed with 400 µl ZR-Duet lysis buffer per 5×10^6 cells, and processed with the ZR-Duet DNA/RNA purification kit (Zymo Research). Each 20 µl qPCR reaction contained: 1× Roche Lightcycler 480 Probes Hot-start Mastermix, 200 nM primers (Quick-LC purified primers; Eurofins MWG Operon), 100 nM Roche UPL hydrolysis probe, and 700 ng template DNA. Cycling conditions on the Lightcycler 480-II qPCR cycler (Roche) were: Taq activation at 95°C for 10 min, followed by 55 cycles of (95°C for 15 s; 60°C for 45 s), using the following primers: CMV long noncoding RNA β2.7: (forward, 5′-TGTTCTTCTGGTTCATTTCCTATG-3′; reverse, 5′-CGTGTCCGGTCCTGATTC-3′; probe, GGCTGCTG); CMV UL69 (forward, 5′-CCTACGACTTTCGGTTCT TCTC-3′; reverse, 5′-CGTCCAGTTCGTCGTCAATAA-3′; probe, CCTCAGCC), cellular genomic RNase P primers (forward, 5′-GACGGACTGCGCAGGTTA-3′; reverse, 5′-CCATGCTGAAGTCCCATGA-3′; probe, CAGCTCCC). These RNAβ 2.7 and UL69 primers were chosen and optimized to ensure that they function with maximum specificity and sensitivity. The genomes of 100 clinical CMV strains were aligned to generate multiple primers to amplify the most highly conserved regions across the CMV genome. Primers were tested for on sequences from uninfected cells with low levels of "spiked" viral genomes, and primers for were chosen based on specificity and sensitivity that exceeded that used in clinical protocols (Binnicker and Espy, 2013). Total cellular genomes were quantitated using a standard curve of known cellular genome concentration amplified using primers for human RNase P: RPP30. CMV genomes were quantitated using a standard concentration curve of SwaI-linearized HCMV BAC genomes (strain TB40/E, available from Gen-Bank under accession no. EF999921.1), diluted in 5 ng/µl sonicated salmon sperm carrier DNA (Ambion). Each sample was run in 10–13 replicates and scored as "detected" (CMV genome target[s] detected in any replicate) or "not detected" (no CMV genome targets detected in any replicate). The limit of detection for the RNase P and β2.7 genes was 1–2

copies and 100 genomes, respectively. Negative controls included water, 5 ng/µl sheared salmon sperm carrier DNA, or genomes extracted from cultured uninfected primary cells (MRC-5; CCL-171; ATCC).

Statistical analysis
Descriptive statistics (percent means, standard deviations, counts) were calculated using Microsoft Excel. P-values for comparison of means within each tissue site were determined by Student's t test and corrected using Holm–Sidak for multiple comparisons. Frequency variance for CMV-specific TEM cells was determined for each tissue by Holm–Sidak posthoc multiple comparison after two-way ANOVA in PRISM (GraphPad Software, Inc.). Linear regression of age and T cell subset distribution was also performed in PRISM. Slopes of regression lines and y intercepts were compared. Statistical significance was defined as $P < 0.05$.

Online supplemental material
Fig. S1 shows gating strategies. Table S1 lists tissues acquired from individual CMV seropositive donors. Table S2 is a list of CMV-specific and control multimer reagents used for analysis of human T cells. Table S3 lists characteristics of organ donors used for Figs. 6 and 7. Table S4, List of fluorochrome-conjugated antibodies and flow cytometry reagents used in this study.

REFERENCES

Adland, E., P. Klenerman, P. Goulder, and P.C. Matthews. 2015. Ongoing burden of disease and mortality from HIV/CMV coinfection in Africa in the antiretroviral therapy era. *Front. Microbiol.* 6:1016. http://dx.doi .org/10.3389/fmicb.2015.01016

Akulian, J.A., M.R. Pipeling, E.R. John, J.B. Orens, N. Lechtzin, and J.F. McDyer. 2013. High-quality CMV-specific CD4+ memory is enriched in the lung allograft and is associated with mucosal viral control. *Am. J. Transplant.* 13:146–156. http://dx.doi.org/10.1111/j.1600-6143.2012 .04282.x

Anderson, K.G., H. Sung, C.N. Skon, L. Lefrancois, A. Deisinger, V. Vezys, and D. Masopust. 2012. Cutting edge: intravascular staining redefines lung CD8 T cell responses. *J. Immunol.* 189:2702–2706. http://dx.doi.org/10 .4049/jimmunol.1201682

Arens, R., E.B. Remmerswaal, J.A. Bosch, and R.A. van Lier. 2015. 5(th) International Workshop on CMV and Immunosenescence – A shadow of cytomegalovirus infection on immunological memory. *Eur. J. Immunol.* 45:954–957. http://dx.doi.org/10.1002/eji.201570044

Betts, M.R., J.M. Brenchley, D.A. Price, S.C. De Rosa, D.C. Douek, M. Roederer, and R.A. Koup. 2003. Sensitive and viable identification of antigen-specific CD8+ T cells by a flow cytometric assay for degranulation. *J. Immunol. Methods.* 281:65–78. http://dx.doi.org/10 .1016/S0022-1759(03)00265-5

Bingaman, A.W., D.S. Patke, V.R. Mane, M. Ahmadzadeh, M. Ndjembi, S.T. Bartlett, and D.L. Farber. 2005. Novel phenotypes and migratory properties distinguish memory CD4 T cell subsets in lymphoid and lung tissue. *Eur. J. Immunol.* 35:3173–3186. http://dx.doi.org/10.1002/eji .200526004

Binnicker, M.J., and M.E. Espy. 2013. Comparison of six real-time PCR assays for qualitative detection of cytomegalovirus in clinical specimens. *J. Clin. Microbiol.* 51:3749–3752. http://dx.doi.org/10.1128/JCM.02005 -13

Borchers, S., J. Ogonek, P.R. Varanasi, S. Tischer, M. Bremm, B. Eiz-Vesper, U. Koehl, and E.M. Weissinger. 2014. Multimer monitoring of CMV-specific T cells in research and in clinical applications. *Diagn. Microbiol. Infect. Dis.* 78:201–212. http://dx.doi.org/10.1016/j.diagmicrobio.2013 .11.007

Chidrawar, S., N. Khan, W. Wei, A. McLarnon, N. Smith, L. Nayak, and P. Moss. 2009. Cytomegalovirus-seropositivity has a profound influence on the magnitude of major lymphoid subsets within healthy individuals. *Clin. Exp. Immunol.* 155:423–432. http://dx.doi.org/10.1111/j.1365 -2249.2008.03785.x

Cook, C.H., and J. Trgovcich. 2011. Cytomegalovirus reactivation in critically ill immunocompetent hosts: a decade of progress and remaining challenges. *Antiviral Res.* 90:151–159. http://dx.doi.org/10.1016/j .antiviral.2011.03.179

de Bree, G.J., E.M. van Leeuwen, T.A. Out, H.M. Jansen, R.E. Jonkers, and R.A. van Lier. 2005. Selective accumulation of differentiated CD8+ T cells specific for respiratory viruses in the human lung. *J. Exp. Med.* 202:1433–1442. http://dx.doi.org/10.1084/jem.20051365

Di Benedetto, S., E. Derhovanessian, E. Steinhagen-Thiessen, D. Goldeck, L. Müller, and G. Pawelec. 2015. Impact of age, sex and CMV-infection on peripheral T cell phenotypes: results from the Berlin BASE-II Study. *Biogerontology.* 16:631–643. http://dx.doi.org/10.1007/s10522-015 -9563-2

Frantzeskaki, F.G., E.S. Karampi, C. Kottaridi, M. Alepaki, C. Routsi, M. Tzanela, D.A. Vassiliadi, E. Douka, E. Tsaousi, V. Gennimata, et al. 2015. Cytomegalovirus reactivation in a general, nonimmunosuppressed intensive care unit population: incidence, risk factors, associations with organ dysfunction, and inflammatory biomarkers. *J. Crit. Care.* 30:276–281. http://dx.doi.org/10.1016/j.jcrc.2014.10.002

Furman, D., V. Jojic, S. Sharma, S.S. Shen-Orr, C.J. Angel, S. Onengut-Gumuscu, B.A. Kidd, H.T. Maecker, P. Concannon, C.L. Dekker, et

al. 2015. Cytomegalovirus infection enhances the immune response to influenza. *Sci. Transl. Med.* 7:281ra43. http://dx.doi.org/10.1126/ scitranslmed.aaa2293

Gamadia, L.E., R.J. Rentenaar, P.A. Baars, E.B. Remmerswaal, S. Surachno, J.F. Weel, M. Toebes, T.N. Schumacher, I.J. ten Berge, and R.A. van Lier. 2001. Differentiation of cytomegalovirus-specific CD8+ T cells in healthy and immunosuppressed virus carriers. *Blood.* 98:754–761. http ://dx.doi.org/10.1182/blood.V98.3.754

Ganusov, V.V., and R.J. De Boer. 2007. Do most lymphocytes in humans really reside in the gut? *Trends Immunol.* 28:514–518. http://dx.doi.org /10.1016/j.it.2007.08.009

Gebhardt, T., L.M. Wakim, L. Eidsmo, P.C. Reading, W.R. Heath, and F.R. Carbone. 2009. Memory T cells in nonlymphoid tissue that provide enhanced local immunity during infection with herpes simplex virus. *Nat. Immunol.* 10:524–530. http://dx.doi.org/10.1038/ni.1718

Goodrum, F. 2016. Human cytomegalovirus latency: approaching the Gordian knot. *Annu Rev Virol.* 3:333–357. http://dx.doi.org/10.1146/ annurev-virology-110615-042422

Goodrum, F., K. Caviness, and P. Zagallo. 2012. Human cytomegalovirus persistence. *Cell. Microbiol.* 14:644–655. http://dx.doi.org/10.1111/j .1462-5822.2012.01774.x

Hahn, G., R. Jores, and E.S. Mocarski. 1998. Cytomegalovirus remains latent in a common precursor of dendritic and myeloid cells. *Proc. Natl. Acad. Sci. USA.* 95:3937–3942. http://dx.doi.org/10.1073/pnas.95.7.3937

Hakki, M., S.R. Riddell, J. Storek, R.A. Carter, T. Stevens-Ayers, P. Sudour, K. White, L. Corey, and M. Boeckh. 2003. Immune reconstitution to cytomegalovirus after allogeneic hematopoietic stem cell transplantation: impact of host factors, drug therapy, and subclinical reactivation. *Blood.* 102:3060–3067. http://dx.doi.org/10.1182/blood-2002-11-3472

Iijima, N., and A. Iwasaki. 2014. T cell memory. A local macrophage chemokine network sustains protective tissue-resident memory CD4 T cells. *Science.* 346:93–98. http://dx.doi.org/10.1126/science.1257530

Jiang, X., R.A. Clark, L. Liu, A.J. Wagers, R.C. Fuhlbrigge, and T.S. Kupper. 2012. Skin infection generates non-migratory memory CD8+ T(RM) cells providing global skin immunity. *Nature.* 483:227–231. http://dx .doi.org/10.1038/nature10851

Kivisäkk, P., D.J. Mahad, M.K. Callahan, C. Trebst, B. Tucky, T. Wei, L. Wu, E.S. Baekkevold, H. Lassmann, S.M. Staugaitis, et al. 2003. Human cerebrospinal fluid central memory CD4+ T cells: evidence for trafficking through choroid plexus and meninges via P-selectin. *Proc. Natl. Acad. Sci. USA.* 100:8389–8394. http://dx.doi.org/10.1073/pnas.1433000100

Kotton, C.N., D. Kumar, A.M. Caliendo, A. Asberg, S. Chou, L. Danziger-Isakov, and A. Humar. Transplantation Society International CMV Consensus Group. 2013. Updated international consensus guidelines on the management of cytomegalovirus in solid-organ transplantation. *Transplantation.* 96:333–360. http://dx.doi.org/10.1097/TP .0b013e31829df29d

Laugel, B., H.A. van den Berg, E. Gostick, D.K. Cole, L. Wooldridge, J. Boulter, A. Milicic, D.A. Price, and A.K. Sewell. 2007. Different T cell receptor affinity thresholds and CD8 coreceptor dependence govern cytotoxic T lymphocyte activation and tetramer binding properties. *J. Biol. Chem.* 282:23799–23810. http://dx.doi.org/10.1074/jbc.M700976200

Letsch, A., M. Knoedler, I.K. Na, F. Kern, A.M. Asemissen, U. Keilholz, M. Loesch, E. Thiel, H.D. Volk, and C. Scheibenbogen. 2007. CMV-specific central memory T cells reside in bone marrow. *Eur. J. Immunol.* 37:3063–3068. http://dx.doi.org/10.1002/eji.200636930

Libri, V., R.I. Azevedo, S.E. Jackson, D. Di Mitri, R. Lachmann, S. Fuhrmann, M. Vukmanovic-Stejic, K. Yong, L. Battistini, F. Kern, et al. 2011. Cytomegalovirus infection induces the accumulation of short-lived, multifunctional CD4+CD45RA+CD27+ T cells: the potential involvement of interleukin-7 in this process. *Immunology.* 132:326–339. http://dx.doi.org/10.1111/j.1365-2567.2010.03386.x

Lichtner, M., P. Cicconi, S. Vita, A. Cozzi-Lepri, M. Galli, S. Lo Caputo, A. Saracino, A. De Luca, M. Moioli, F. Maggiolo, et al. ICONA Foundation Study. 2015. Cytomegalovirus coinfection is associated with an increased risk of severe non–AIDS-defining events in a large cohort of HIV-infected patients. *J. Infect. Dis.* 211:178–186. http://dx.doi.org/10.1093/infdis/jiu417

Liu, L., Q. Zhong, T. Tian, K. Dubin, S.K. Athale, and T.S. Kupper. 2010. Epidermal injury and infection during poxvirus immunization is crucial for the generation of highly protective T cell-mediated immunity. *Nat. Med.* 16:224–227. http://dx.doi.org/10.1038/nm.2078

Ljungman, P., M. Hakki, and M. Boeckh. 2010. Cytomegalovirus in hematopoietic stem cell transplant recipients. *Infect. Dis. Clin. North Am.* 24:319–337. http://dx.doi.org/10.1016/j.idc.2010.01.008

Masopust, D., V. Vezys, A.L. Marzo, and L. Lefrançois. 2001. Preferential localization of effector memory cells in nonlymphoid tissue. *Science.* 291:2413–2417. http://dx.doi.org/10.1126/science.1058867

Masopust, D., V. Vezys, E.J. Usherwood, L.S. Cauley, S. Olson, A.L. Marzo, R.L. Ward, D.L. Woodland, and L. Lefrançois. 2004. Activated primary and memory CD8 T cells migrate to nonlymphoid tissues regardless of site of activation or tissue of origin. *J. Immunol.* 172:4875–4882. http://dx.doi.org/10.4049/jimmunol.172.8.4875

Masopust, D., V. Vezys, E.J. Wherry, D.L. Barber, and R. Ahmed. 2006. Cutting edge: gut microenvironment promotes differentiation of a unique memory CD8 T cell population. *J. Immunol.* 176:2079–2083. http://dx.doi.org/10.4049/jimmunol.176.4.2079

Miller, J.D., R.G. van der Most, R.S. Akondy, J.T. Glidewell, S. Albott, D. Masopust, K. Murali-Krishna, P.L. Mahar, S. Edupuganti, S. Lalor, et al. 2008. Human effector and memory CD8+ T cell responses to smallpox and yellow fever vaccines. *Immunity.* 28:710–722. http://dx.doi.org/10.1016/j.immuni.2008.02.020

Palendira, U., R. Chinn, W. Raza, K. Piper, G. Pratt, L. Machado, A. Bell, N. Khan, A.D. Hislop, R. Steyn, et al. 2008. Selective accumulation of virus-specific CD8+ T cells with unique homing phenotype within the human bone marrow. *Blood.* 112:3293–3302. http://dx.doi.org/10.1182/blood-2008-02-138040

Pera, A., C. Campos, A. Corona, B. Sanchez-Correa, R. Tarazona, A. Larbi, and R. Solana. 2014. CMV latent infection improves CD8+ T response to SEB due to expansion of polyfunctional CD57+ cells in young individuals. *PLoS One.* 9:e88538. http://dx.doi.org/10.1371/journal.pone.0088538

Polić, B., H. Hengel, A. Krmpotić, J. Trgovcich, I. Pavić, P. Luccaronin, S. Jonjić, and U.H. Koszinowski. 1998. Hierarchical and redundant lymphocyte subset control precludes cytomegalovirus replication during latent infection. *J. Exp. Med.* 188:1047–1054. http://dx.doi.org/10.1084/jem.188.6.1047

Poole, E., J.K. Juss, B. Krishna, J. Herre, E.R. Chilvers, and J. Sinclair. 2015. Alveolar macrophages isolated directly from human cytomegalovirus (HCMV)-seropositive individuals are sites of HCMV reactivation in vivo. *J. Infect. Dis.* 211:1936–1942. http://dx.doi.org/10.1093/infdis/jiu837

Reeves, M.B., and J.H. Sinclair. 2013. Circulating dendritic cells isolated from healthy seropositive donors are sites of human cytomegalovirus reactivation in vivo. *J. Virol.* 87:10660–10667. http://dx.doi.org/10.1128/JVI.01539-13

Remmerswaal, E.B., S.H. Havenith, M.M. Idu, E.M. van Leeuwen, K.A. van Donselaar, A. Ten Brinke, N. van der Bom-Baylon, F.J. Bemelman, R.A. van Lier, and I.J. Ten Berge. 2012. Human virus-specific effector-type T cells accumulate in blood but not in lymph nodes. *Blood.* 119:1702–1712. http://dx.doi.org/10.1182/blood-2011-09-381574

Santos, C.A., D.C. Brennan, R.D. Yusen, and M.A. Olsen. 2015. Incidence, risk factors and outcomes of delayed-onset cytomegalovirus disease in a large retrospective cohort of lung transplant recipients. *Transplantation.* 99:1658–1666. http://dx.doi.org/10.1097/TP.0000000000000549

Sathaliyawala, T., M. Kubota, N. Yudanin, D. Turner, P. Camp, J.J. Thome, K.L. Bickham, H. Lerner, M. Goldstein, M. Sykes, et al. 2013. Distribution and compartmentalization of human circulating and tissue-resident memory T cell subsets. *Immunity.* 38:187–197. http://dx.doi.org/10.1016/j.immuni.2012.09.020

Sauce, D., M. Larsen, A.M. Leese, D. Millar, N. Khan, A.D. Hislop, and A.B. Rickinson. 2007. IL-7R alpha versus CCR7 and CD45 as markers of virus-specific CD8+ T cell differentiation: contrasting pictures in blood and tonsillar lymphoid tissue. *J. Infect. Dis.* 195:268–278. http://dx.doi.org/10.1086/510248

Schenkel, J.M., K.A. Fraser, L.K. Beura, K.E. Pauken, V. Vezys, and D. Masopust. 2014. T cell memory. Resident memory CD8 T cells trigger protective innate and adaptive immune responses. *Science.* 346:98–101. http://dx.doi.org/10.1126/science.1254536

Slobedman, B., and E.S. Mocarski. 1999. Quantitative analysis of latent human cytomegalovirus. *J. Virol.* 73:4806–4812.

Smith, C.J., S. Caldeira-Dantas, H. Turula, and C.M. Snyder. 2015. Murine CMV infection induces the continuous production of mucosal resident T cells. *Cell Reports.* 13:1137–1148. http://dx.doi.org/10.1016/j.celrep.2015.09.076

Sridhar, S., S. Begom, A. Bermingham, K. Hoschler, W. Adamson, W. Carman, T. Bean, W. Barclay, J.J. Deeks, and A. Lalvani. 2013. Cellular immune correlates of protection against symptomatic pandemic influenza. *Nat. Med.* 19:1305–1312. http://dx.doi.org/10.1038/nm.3350

Teijaro, J.R., D. Turner, Q. Pham, E.J. Wherry, L. Lefrançois, and D.L. Farber. 2011. Cutting edge: Tissue-retentive lung memory CD4 T cells mediate optimal protection to respiratory virus infection. *J. Immunol.* 187:5510–5514. http://dx.doi.org/10.4049/jimmunol.1102243

Thom, J.T., T.C. Weber, S.M. Walton, N. Torti, and A. Oxenius. 2015. The salivary gland acts as a sink for tissue-resident memory CD8+ T cells, facilitating protection from local cytomegalovirus infection. *Cell Reports.* 13:1125–1136. http://dx.doi.org/10.1016/j.celrep.2015.09.082

Thome, J.J., N. Yudanin, Y. Ohmura, M. Kubota, B. Grinshpun, T. Sathaliyawala, T. Kato, H. Lerner, Y. Shen, and D.L. Farber. 2014. Spatial map of human T cell compartmentalization and maintenance over decades of life. *Cell.* 159:814–828. http://dx.doi.org/10.1016/j.cell.2014.10.026

Thome, J.J., K.L. Bickham, Y. Ohmura, M. Kubota, N. Matsuoka, C. Gordon, T. Granot, A. Griesemer, H. Lerner, T. Kato, and D.L. Farber. 2016. Early-life compartmentalization of human T cell differentiation and regulatory function in mucosal and lymphoid tissues. *Nat. Med.* 22:72–77. http://dx.doi.org/10.1038/nm.4008

Tokoyoda, K., S. Zehentmeier, A.N. Hegazy, I. Albrecht, J.R. Grün, M. Löhning, and A. Radbruch. 2009. Professional memory CD4+ T lymphocytes preferentially reside and rest in the bone marrow. *Immunity.* 30:721–730. http://dx.doi.org/10.1016/j.immuni.2009.03.015

Turner, D.L., K.L. Bickham, J.J. Thome, C.Y. Kim, F. D'Ovidio, E.J. Wherry, and D.L. Farber. 2014. Lung niches for the generation and maintenance of tissue-resident memory T cells. *Mucosal Immunol.* 7:501–510. http://dx.doi.org/10.1038/mi.2013.67

Vallejo, A.N., J.C. Brandes, C.M. Weyand, and J.J. Goronzy. 1999. Modulation of CD28 expression: distinct regulatory pathways during activation and replicative senescence. *J. Immunol.* 162:6572–6579.

Wakim, L.M., A. Woodward-Davis, and M.J. Bevan. 2010. Memory T cells persisting within the brain after local infection show functional adaptations to their tissue of residence. *Proc. Natl. Acad. Sci. USA.* 107:17872–17879. http://dx.doi.org/10.1073/pnas.1010201107

Wherry, E.J., V. Teichgräber, T.C. Becker, D. Masopust, S.M. Kaech, R. Antia, U.H. von Andrian, and R. Ahmed. 2003. Lineage relationship and protective immunity of memory CD8 T cell subsets. *Nat. Immunol.* 4:225–234. http://dx.doi.org/10.1038/ni889

Xu, R.H., M. Fang, A. Klein-Szanto, and L.J. Sigal. 2007. Memory CD8+ T cells are gatekeepers of the lymph node draining the site of viral infection. *Proc. Natl. Acad. Sci. USA.* 104:10992–10997. http://dx.doi.org/10.1073/pnas.0701822104